Supporting Information for

High Initial Reversible Capacity and Long Life of Ternary SnO_2-Co-Carbon Nanocomposite Anodes for Lithium-Ion Batteries

Pan Deng[1], Jing Yang[1], Shengyang Li[1], Tian-E Fan[2,*], Hong-Hui Wu[3], Yun Mou[4], Hui Huang[1], Qiaobao Zhang[1,*], Dong-Liang Peng[1], Baihua Qu[1,*]

[1]Pen-Tung Sah Institute of Micro-Nano Science and Technology, and Department of Materials Science and Engineering, College of Materials, Xiamen University, Xiamen 361005, People's Republic of China

[2]College of Automation and Key Laboratory of Industrial Internet of Things and Networked Control, Ministry of Education, Chongqing University of Posts and Telecommunications, Chongqing 400065, People's Republic of China

[3]Department of Chemistry, University of Nebraska-Lincoln, NE 68588 Lincoln, United States

[4]School of Mechanical Science and Engineering, Huazhong University of Science and Technology, Wuhan 430074, People's Republic of China

*Corresponding authors. E-mail: bhqu@xmu.edu.cn (Baihua Qu); fante@cqupt.edu.cn (Tian-E Fan); zhangqiaobao@xmu.edu.cn (Qiaobao Zhang)

Supplementary Figures and Tables

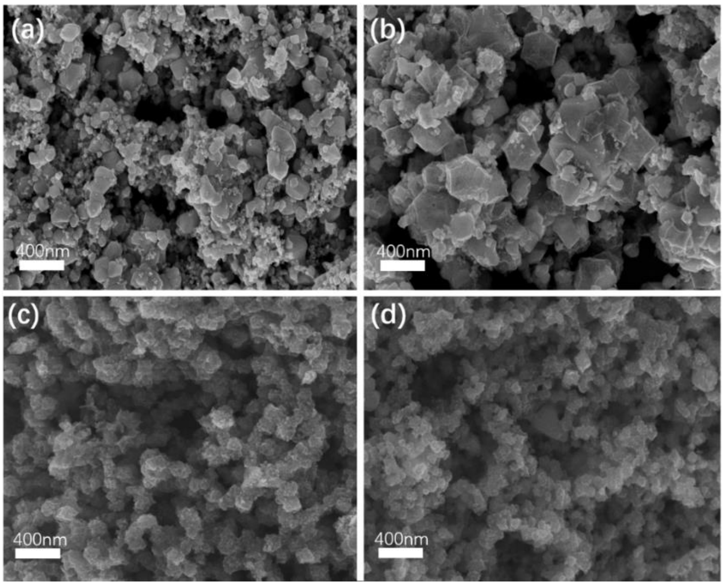

Fig. S1 Morphology of **a** pure SnO_2; **b** N-c-SSC-1; **c** N-c-SSC-2; **d** N-c-SSC-3

The morphology of the commercial SnO_2, N-c-SSC at the ratio of 1.25 mmol-$Co(NO_3)_2{\cdot}6H_2O$ and 5mmol-2-Mi (N-c-SSC-1), N-c-SSC at the ratio of 1.25 mmol-$Co(NO_3)_2{\cdot}6H_2O$ and 10mmol-2-Mi (N-c-SSC-2), N-c-SSC at the ratio of 2 mmol-$Co(NO_3)_2{\cdot}6H_2O$ and 20mmol-2-Mi (N-c-SSC-3) were observed by scanning electron microscope (FESEM) as shown in Fig. S1. The pure SnO_2 particles shows irregular shape with different morphologies in Fig. S1a. After adding ZIF-67, the frameworks of ZIF-67 can be observed in Fig. S1b-d. When the ratio of $Co(NO_3)_2{\cdot}6H_2O$ and 2-Mi is 1:4, the frameworks exhibit bigger (~600 nm) compared to that (~250 nm) in Fig. S1c, d. in which the morphology is a melange of regular frameworks and irregular commercial SnO_2 particles, and the commercial SnO_2 are attached to the frameworks. It comes out quite different that much more uniform particles are obtained when the ratio is 1:8, both of Fig. S1c and S1d exhibit the same polyhedral structure, the irregular SnO_2 particles disappear due to the shield of the small frameworks. Also, smaller nanoparticles can be noticed on the frameworks in Fig. S1c, which doesn't seem so obvious in Fig. S1d. This may be related to the higher carbon content.

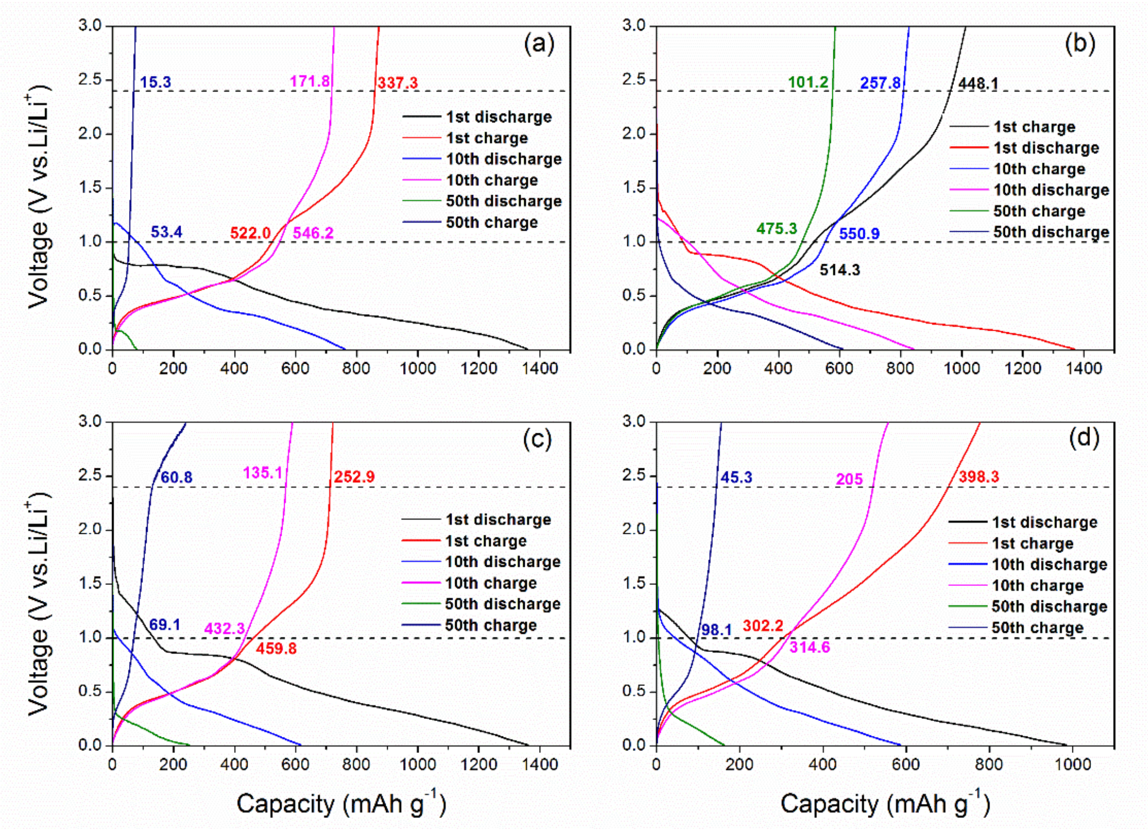

Fig. S2 Charge and discharge curves of **a** commercial SnO_2, **b** N-c-SCC-1, **c** N-c-SCC-2 and **d** N-c-SCC 3 electrodes cycled between 0.01 and 3 V at 0.2 A g^{-1}

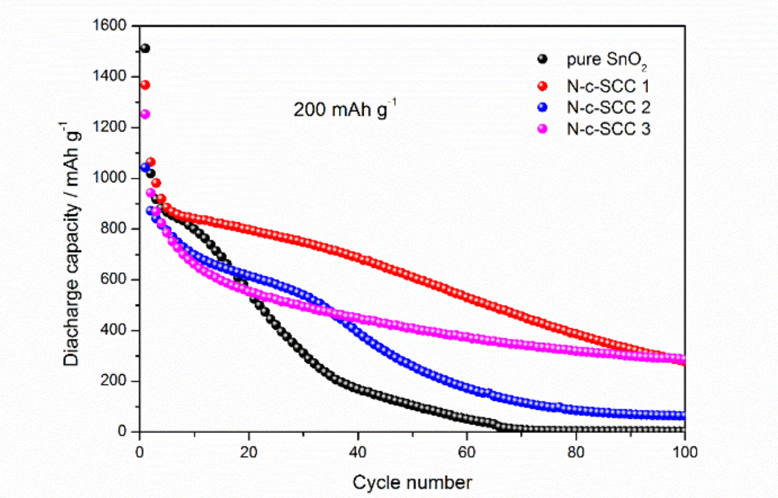

Fig. S3 Cycling performance of the commercial SnO_2 and N-c-SCC electrodes at a current density of 0.2 A g^{-1}

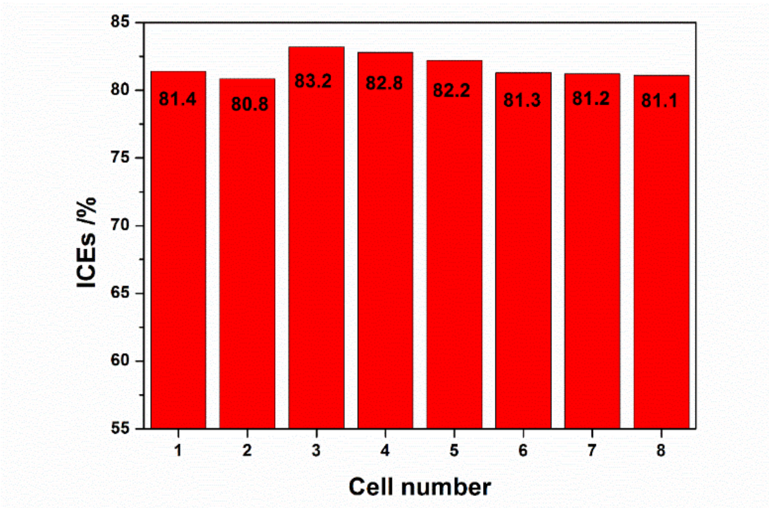

Fig. S4 Statistical ICE of some typical cells

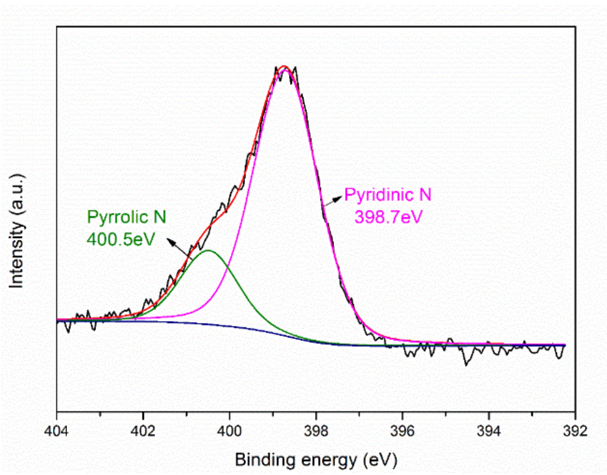

Fig. S5 High-resolution XPS spectra of N1s in N-u-SCC-2 composite

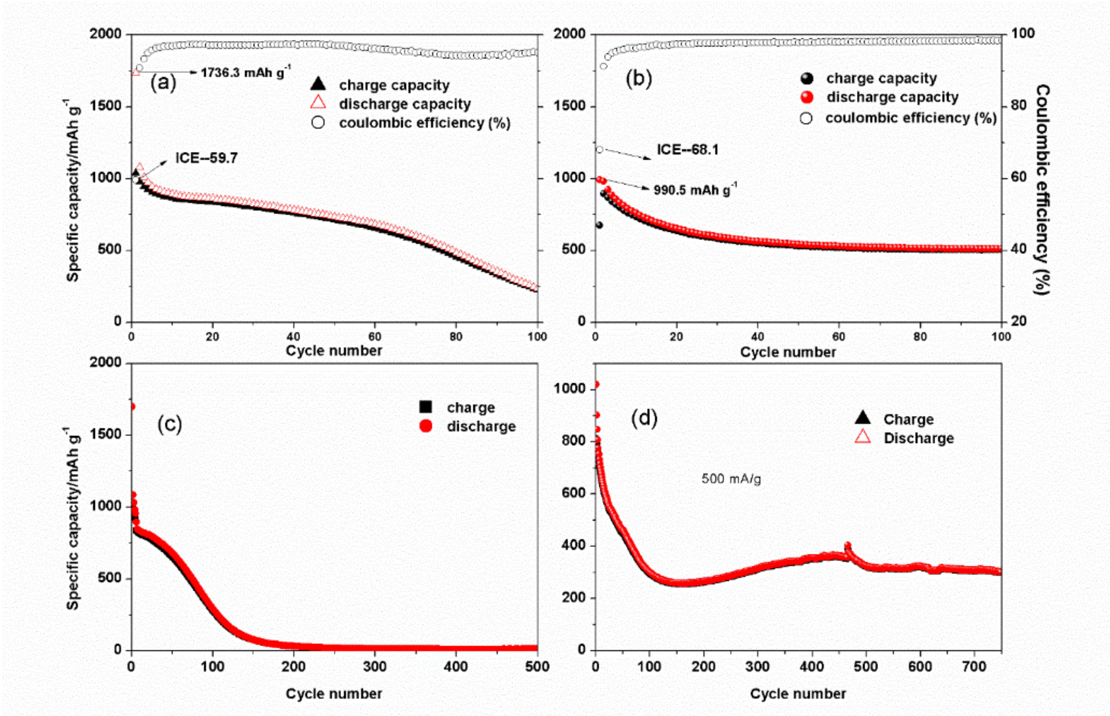

Fig. S6 Cycling performance of **a** ultrafine SnO_2 electrode at a current density of 0.2 A g^{-1}, **b** N-u-SCC-1 electrodes at a current density of 0.2 A g^{-1}, **c** ultrafine SnO_2 electrode at a current density of 0.5 A g^{-1}, **d** N-u-SCC-1 electrodes at a current density of 0.5 A g^{-1}

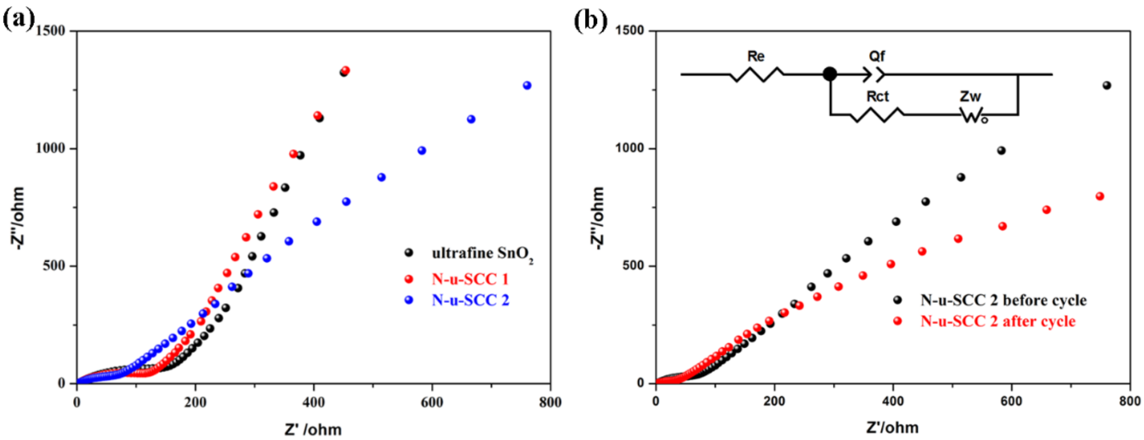

Fig. S7 a Nyquist plots of the three ultrafine SnO_2, N-u-SCC-1, N-u-SCC-2 electrodes. **B** Nyquist plots of N-u-SCC-2 electrodes before and after 100 cycles and the proposed equivalent circuit to fit the impedance data

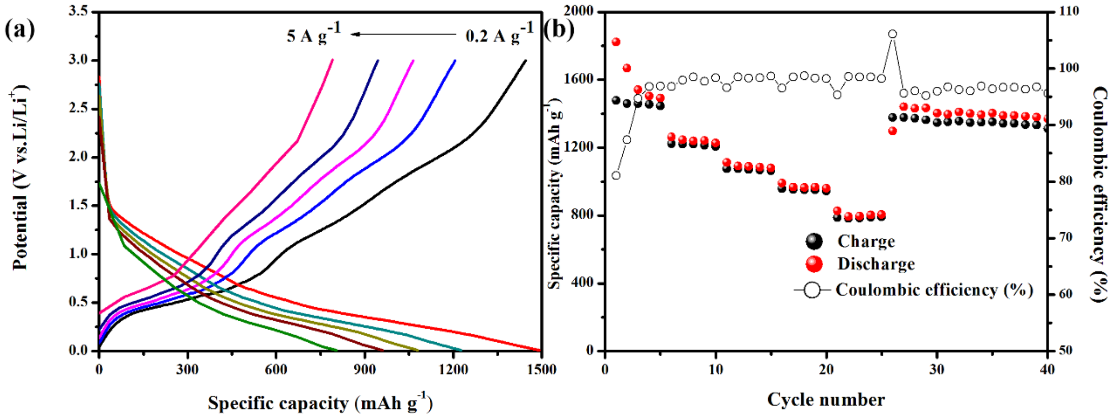

Fig. S8 **a** Discharge/charge curves at different current densities of the N-u-SCC-2 electrode. **b** Rate performance of the N-u-SCC-2 electrode

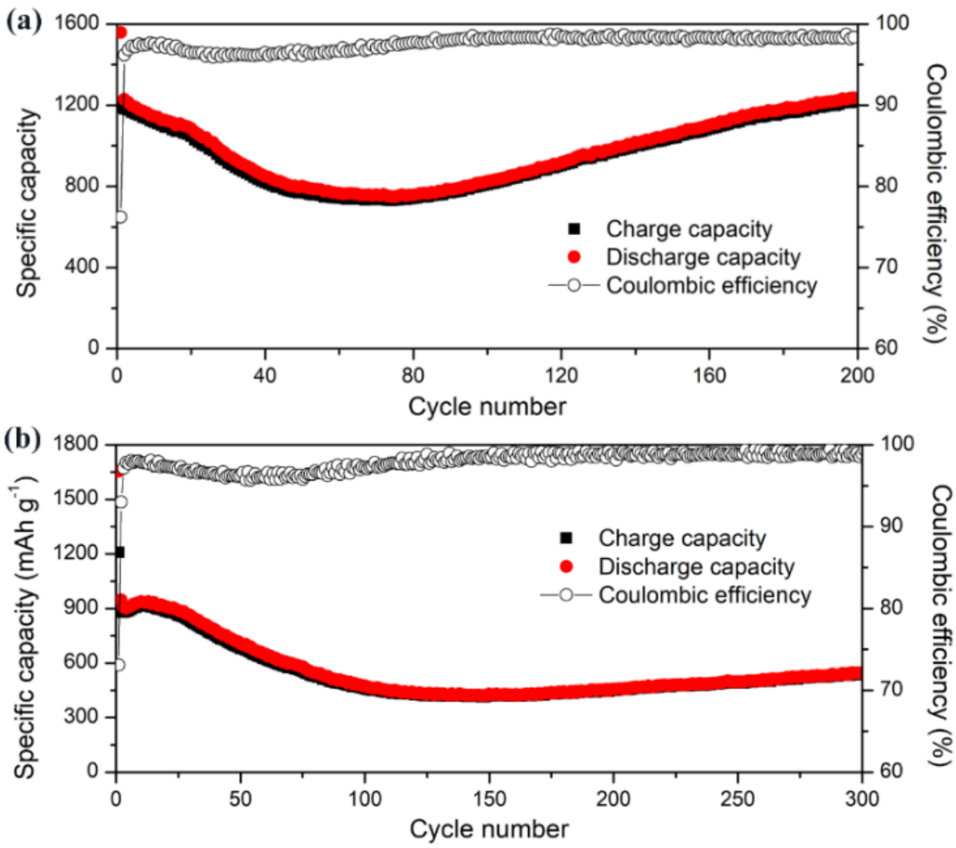

Fig. S9 Cycling performance of the N-u-scc-2 electrode at a current density of **a** 1 A g^{-1} and **b** 2 A g^{-1}

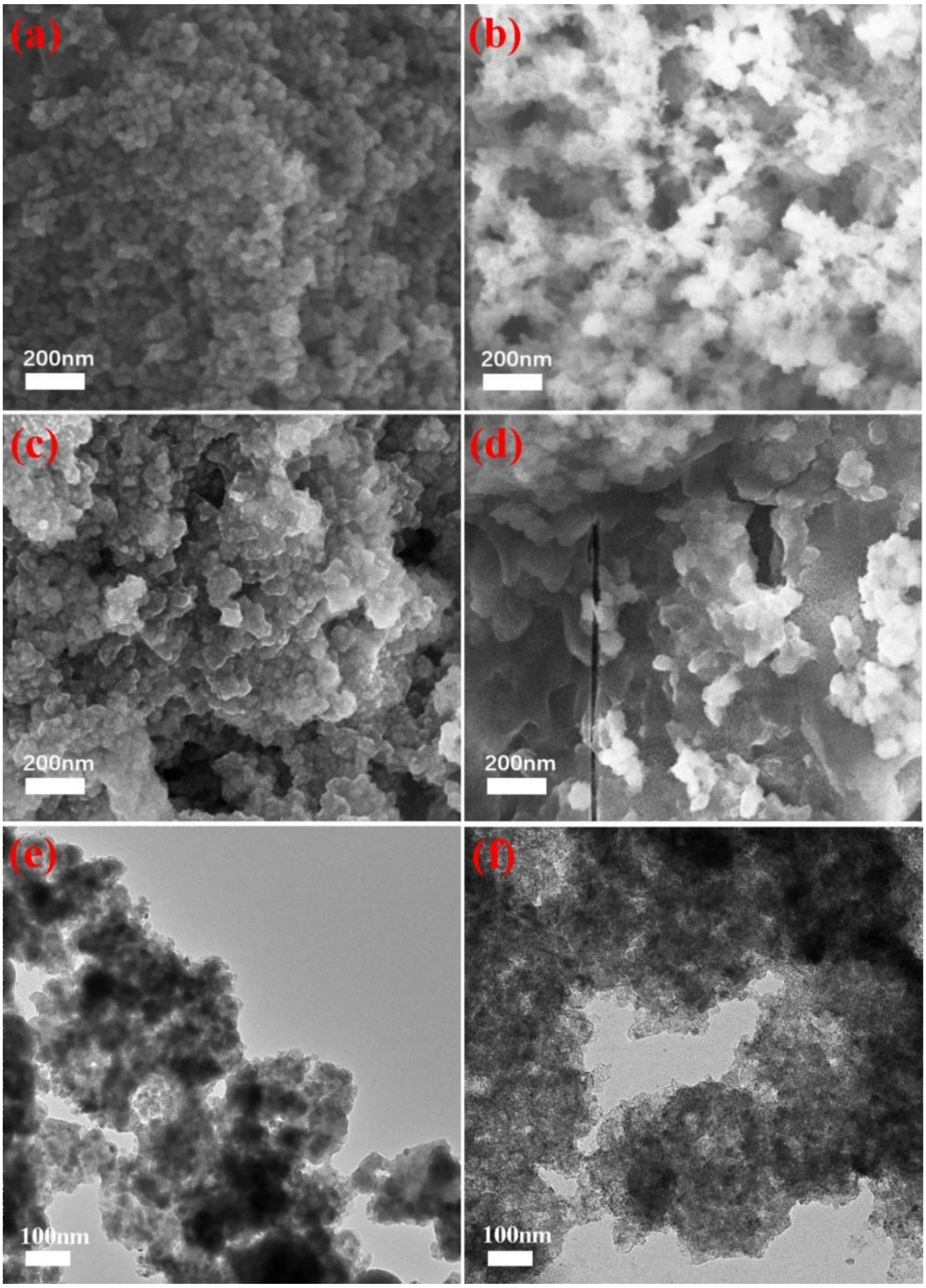

Fig. S10 FESEM image of pure ultrafine SnO_2 **a** before and **b** after 100 cycled, of N-u-SCC 2 **c** before and **d** after 100 cycled. TEM images of N-u-SCC 2 **e** before and **f** after discharging to 1.0 V

Table S1 Part of basic facts of the N-c-SCC composites

Defined name	Mole dosage of $Co(NO_3)_2 \cdot 6H_2O$ (mmol)	Mole dosage of 2-Melm (mmol)	ICE (%)
N-c-SCC-1	1.25	5	
N-c-SCC-2	1.25	10	72.5
N-c-SCC-3	2.5	20	

Table 1 lists synthetic formula and ICE about the three N-c-SCC composites.

Table S2 EDS results of the two N-u-SCC composites

N-u-SCC-1			N-u-SCC-2		
element	Atomic fraction (%)	Mass fraction (%)	element	Atomic fraction (%)	Mass fraction (%)
C	17.21	5.43	C	23.97	9.68
N	19.24	6.93	N	21.23	9.80
O	25.73	11.00	O	33.70	18.46
Co	19.02	25.12	Co	6.63	11.23
Sn	18.80	51.53	Sn	14.48	50.83

Table S3 Comparison of the ICEs and electrochemical properties of N-u-SCC-2 with some reported SnO_2/C anode materials for LIBs

Type of composite	ICE (%)	Current density ($A\ g^{-1}$)	Capacity ($mAh\ g^{-1}$)	cycles	Potential window	Year	Refs.
SnO_2NC@N-RGO	61.3	0.5	1346	500	0.005-3 V	2013	[1]
Bowl-like SnO_2@C	68.4	0.4	963	100	0.005-3.0 V	2014	[2]
Core-shell SnO_2/C	69.3	0.1	750	100	0.01-3 V	2015	[3]
SnO_2@N-CNF	69.2	0.1	754@1 $A\ g^{-1}$	300	0.01-3 V	2016	[4]
SnO_2/NC	51	0.5	491	100	0.01-2 V	2016	[5]
SnO_2/Co@C	66	0.2	800	100	0.01-2.5 V	2017	[6]
PDA-coated SnO_2	61.3	0.16	~1200	300	0.01-3 V	2017	[7]
SnO_2-Mn-G	76.2	0.2	850	400	0.01-3 V	2017	[8]
Porous $SnO_{2-δ}/C$	74.3	0.1	543@1 $A\ g^{-1}$	1000	0.01-3 V	2018	[9]
NuSCC-2	82.2	0.2	975@0.2 $A\ g^{-1}$ 760@0.5 $A\ g^{-1}$	100 400	0.01-3 V	Our work	

Table S4 EIS fitting results of N-u-SCC-2 electrode before and after cycling

Element	Value 1 (before cycling)	Value 2 (after 100 cycling)
*R*e	0.703	2.785
*R*ct	179	32.1
*Z*w-R	1.745	3079
*Z*w-T	40.23	5.412
*Z*w-P	0.867	0.640
*Q*ct-T	0.0003	9.11E-05
*Q*ct-P	0.526	0.646

Supplementary References

[1] X. Zhou, L. J. Wan, Y.G. Guo, Binding SnO_2 nanocrystals in nitrogen-doped graphene sheets as anode materials for lithium-ion batteries. Adv. Mater. **25**(15), 2152-2157 (2013). https://doi.org/10.1002/adma.201300071

[2] J. Liang, X.Y. Yu, H. Zhou, H.B. Wu, S. Ding, X.W. Lou, Bowl-like SnO_2 @carbon hollow particles as an advanced anode material for lithium-ion batteries. Angew. Chem. Int. Ed. **53**(47), 12803-12807 (2014). https://doi.org/10.1002/anie.201407917

[3] D. Zhou, W.L. Song, L.Z. Fan, Hollow Core-Shell SnO_2/C Fibers as Highly Stable Anodes for Lithium-Ion Batteries. ACS Appl. Mater. Interfaces **7**(38), 21472-21478 (2015). https://doi.org/10.1021/acsami.5b06512

[4] L. Xia, S. Wang, G. Liu, L. Ding, D. Li, H. Wang, S. Qiao, Flexible SnO_2/N-Doped Carbon Nanofiber Films as Integrated Electrodes for Lithium-Ion Batteries with Superior Rate Capacity and Long Cycle Life. Small **12**(7), 853-859 (2016). https://doi.org/10.1002/smll.201503315

[5] X. Zhou, L. Yu, X.W. Lou, Formation of Uniform N-doped Carbon-Coated SnO_2 Submicroboxes with Enhanced Lithium Storage Properties. Adv. Energy Mater. **6**(14), 1600451 (2016). https://doi.org/10.1002/aenm.201600451

[6] Q. He, J. Liu, Z. Li, Q. Li, L. Xu, B. Zhang, J. Meng, Y. Wu, L. Mai, Solvent-Free Synthesis of Uniform MOF Shell-Derived Carbon Confined SnO_2/Co Nanocubes for Highly Reversible Lithium Storage. Small **13**(37), 1701504 (2017). https://doi.org/10.1002/smll.201701504

[7] B. Jiang, Y. He, B. Li, S. Zhao, S. Wang, Y.B. He, Z. Lin, Polymer-Templated Formation of Polydopamine-Coated SnO_2 Nanocrystals: Anodes for Cyclable Lithium-Ion Batteries. Angew. Chem. Int. Ed. **56**(7), 1869-1872 (2017). https://doi.org/10.1002/anie.201611160

[8] R. Hu, Y. Ouyang, T. Liang, X. Tang, B. Yuan, J. Liu, L. Zhang, L. Yang, M. Zhu, Inhibiting grain coarsening and inducing oxygen vacancies: the roles of Mn in achieving a highly reversible conversion reaction and a long life SnO_2–Mn–graphite ternary anode. Energy Environ. Sci. **10**(9), 2017-2029 (2017). https://doi.org/10.1039/C7EE01635B

[9] R. Jia, J. Yue, Q. Xia, J. Xu, X. Zhu, S. Sun, T. Zhai, H. Xia, Carbon shelled porous $SnO_{2-\delta}$ nanosheet arrays as advanced anodes for lithium-ion batteries. Energy Storage Mater. **13**, 303-311 (2018). https://doi.org/10.1016/j.ensm.2018.02.009